MARSDEN FUND
TE PŪTEA RANGAHAU A MARSDEN
hrc Health Research Council of New Zealand

AUCKLAND BIOENGINEERING INSTITUTE
THE UNIVERSITY OF AUCKLAND NEW ZEALAND

Image-Driven Modelling of Myocardial Fibrosis In Heart Failure

Vicky Y. Wang, Alexander Wilson, Gregory B. Sands, Alistair A. Young, Ian J. LeGrice, Martyn P. Nash

1. Motivation

- Gaining more insights to the mechanisms of heart failure (HF), which can be categorised into diastolic HF (DHF) and systolic HF (SHF).
- Both structural and passive functional remodelling have been observed in the spontaneously hypertensive rat (SHR).
- The relative contributions of geometric remodelling and myocardial fibrosis towards diastolic dysfunction are unknown.
- Utilise image motivated modelling framework to examine the mechanistic link

3. Discussion

- *In vivo* 3D imaging of the SHR hearts confirmed progression of LV from DHF to SHF.
- To examine the relationship between structural and functional remodelling, we developed modelling approach to integrate multiple imaging data.
- We showed that LV hypertrophy alone cannot be responsible for the elevated chamber stiffness in the SHRs.
- Myocardial fibrosis plays a key role in impaired diastolic function. Further analysis is required for investigating systolic dysfunction.

2. Methodology

Step 1: Structural remodelling in HF

- *In vivo* MRI of normal Wistar-Kyoto (WKY) rat and diseased SHR hearts were obtained at 14- and 24-months of age.
- Subject-specific finite element model of the left ventricle (LV) constructed from MRI
- *Ex vivo* confocal images of myocardial tissue blocks were acquired to examine microstructural remodelling.

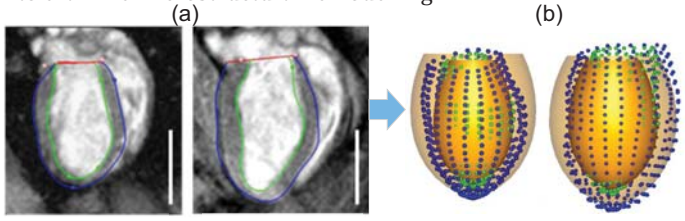

Fig. 1: (a) Long-axis views of *in vivo* MRI of WKY and SHR hearts. (b) Subject-specific LV FE model.

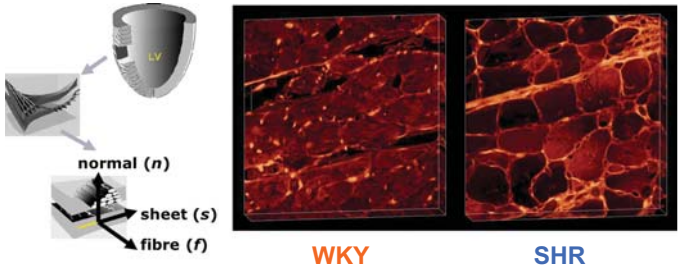

Fig. 2: *Ex vivo* high resolution confocal images of WKY and SHR hearts.

Step 2: Functional remodelling in HF

- *Ex vivo* LV pressure inflation experiment performed on isolated hearts showed changes in LV chamber compliance between normal and diseased and also between the different ages.

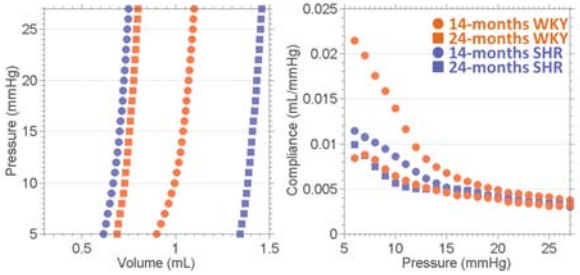

Fig. 3: *Ex vivo* LV pressure-volume and compliance curves for WKY and SHR rat hearts at 14 and 24-months of age.

Step 3: Modelling of passive HF mechanics

- LV passive inflation experiment was simulated using mechanical properties were described using an orthotropic constitutive model.
- Two parameters characterising endomysial (t_{endo}) and perimysial collagen (t_{peri}) thickening were incorporated to take into account the microstructural changes observed in Fig. 2.

$$\bar{W} = \frac{t_{endo}a_f}{2b_f}\left\{\exp\left[b_f(I_{4f}-1)^2\right]-1\right\} + \frac{t_{endo}a_s}{2b_s}\left\{\exp[b_s(I_{4s}-1)^2]-1\right\} + \frac{t_{peri}a_n}{2b_n}\left\{\exp[b_n(I_{4n}-1)^2]-1\right\} + \frac{a_{fs}}{2b_{fs}}\left\{\exp\left[b_{fs}I_{8fs}^2\right]-1\right\}$$

Step 4: Predicting passive tissue properties

- Normal growth correlated with concentric hypertrophy (↑ LV mass, ↓ End-diastolic volume); younger aged SHR exhibited preserved ejection fraction (EF), while older aged SHR developed dilated LV, which led to ↓ EF.

Animal	LV Mass (mg)	EDV (µl)	EF (%)
14-months WKY	794	750	63
24-months WKY	941	631	80
14-months SHR	734	702	52
24-months SHR	1415	789	45

- A single set of material parameters (a_f, a_s, a_n, a_{fs}, b_f, b_n, b_s, and b_{fs}) were estimated to match the subject-specific LV compliance curves for each of the four cases shown in Fig. 3.

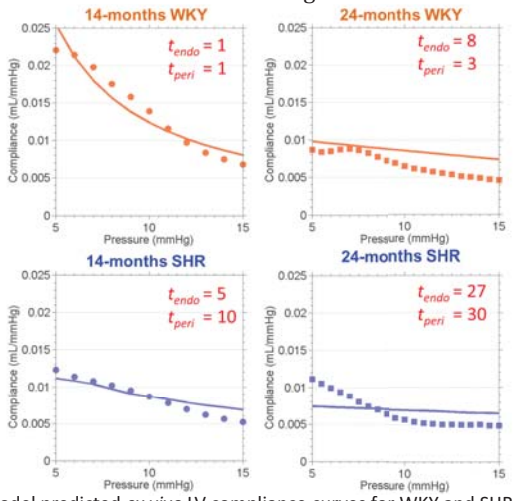

Fig. 4: Model predicted *ex vivo* LV compliance curves for WKY and SHR rat hearts at 14- and 24-moths of age.